Localized glassy behavior in concentrated globular protein solutions driven by intermediate range order

P. D. Godfrin,[1,a)] P. Falus,[2] L. Porcar,[2] K. Hong,[3] S. D. Hudson,[4] N. J. Wagner,[1] and Y. Liu[1,5,b)]

[1]*Center for Neutron Science, Department of Chemical and Biomolecular Engineering, University of Delaware, Newark, DE 19716, USA*

[2]*Institut Laue-Langevin, 38042 Grenoble Cedex 9, France*

[4]*Center for Nanophase Materials and Sciences, Oak Ridge National Laboratory, Oak Ridge, TN 37831, USA*

[5]*Polymers and Complex Fluids Group, National Institute of Standards and Technology, Gaithersburg, MD 20899, USA*

[6]*Center for Neutron Research, National Institute of Standards and Technology, Gaithersburg, MD 20899, USA*

Abstract: Concentrated lysozyme solutions with both a short-ranged attraction and a long-ranged repulsion (SALR) exhibit extremely slow local dynamics, similar to many glassy colloidal systems, due to the locally heterogeneous density distribution at the length scale of intermediate range order. In this paper, we construct a dynamic state diagram for the localized slow dynamics of lysozyme solutions by systematically studying the interaction potential and the short-time dynamics of concentrated lysozyme solutions using small angle neutron scattering, neutron spin echo, and computer simulations. We identified a range of concentrated solutions where the localized glassy behavior can coexist with diffusive long time behavior. The localized glassy like behavior of lysozyme solutions is observed to occur in the random percolated region of the recently proposed generalized phase diagram of SALR systems. This unique dynamic state of a system with the SALR interaction may be a precursor to a macroscopic gel/glass at even higher concentrations.

Material properties of many complex fluids and colloidal suspensions are affected by the solution structure, especially when samples transition from a liquid to a glass or gel state. However, while the glass and gelation transitions of colloidal suspensions have been extensively studied for hard sphere and adhesive hard sphere suspensions,[1–4] the soft matter community still lacks a consensus on the physical origin of dynamic arrest for systems with more complex interaction potentials.[5]

Recently, there are growing interests in studying colloidal systems with both a short-ranged attraction and a long-ranged repulsion (SALR) due to its importance of studying concentrated proteins solutions for the applications such as protein crystallization and pharmaceutical formulation.[6] For some globular proteins with large ionic strength in solution, the thermodynamics can be accurately calculated and predicted based on an isotropic short-ranged attraction.[6–10] However, for solutions with very low ionic strength, the interactions between globular proteins can be accurately represented by a SALR

[a)] Current address: Department of Chemical Engineering, Massachusetts Institute of Technology, Cambridge, MA 02139
[b)] Author to whom correspondence should be addressed. Electronic mail: yunliu@nist.gov or yun.liu@udel.edu

interaction.

Interestingly, the competition between a short-ranged attraction and a long-ranged repulsion produces a diverse landscape of equilibrium and structural arrested states.[11] A recent simulation study established a generalized phase diagram of SALR systems containing a variety of distinguishable liquid states (e.g., dispersed fluid state, random percolated state, clustered fluid state, cluster percolated state) and relating these to an underlying gas-liquid phase transition for a simple reference system.[12] Importantly, this study highlights the role of the long-ranged repulsive interaction potential to frustrate the bulk phase separation driven by the short-range attraction. To explore this unique behavior experimentally, the solution microstructure and protein short-time and long-time dynamics and viscosity in concentrated solutions of a globular protein, lysozyme, at low ionic strength were recently measured.[13] The results revealed that the normalized mean square displacement at short and intermediate time scales of very concentrated solutions is comparable to that of many colloidal glass systems, even though these solutions remain Newtonian with diffusive motions at long time scales. The slow short-time dynamics are due to the formation of intermediate range order (IRO) introduced by the SALR interactions.[12] The competing interactions produce a heterogeneous density distribution at the intermediate range length scale, resulting in localized glassy behavior in high density regions with locally hindered dynamics, while maintaining a freely flowing, homogeneous solution on longer length scales.

In order to further understand the effect of the localized glassy behavior in SALR colloidal systems in general, it is therefore important to determine the state diagram of these localized glassy regions and identify the liquid state in which they exist within the generalized phase diagram. In this paper, we determine the state diagram of the localized glassy dynamics behavior using lysozyme as a model protein system investigated by a combination of small angle neutron scattering (SANS), neutron spin echo (NSE), integral equation theories (IET), and Monte Carlo (MC) computer simulations.

To identify the state points in the proposed generalized phase diagram, we obtain the interaction potential between lysozyme proteins in solution using SANS analyzed with IET and MC simulations. Lysozyme solutions in deuterated water with concentrations from 10 to 480 mg/mL at temperatures ranging from 5 ^{o}C to 50 ^{o}C were measured using SANS and the results are shown in Figure 1. (The sample preparation is described in the supporting information.) Shown in Fig. 1 are the absolute scattering intensities, $I(q)$, normalized by the protein volume fraction, ϕ, after subtracting the background scattering intensity, B. To be consistent with previous studies,[13–15] the volume fraction of these samples are calculated from the weight fractions using the skeleton density unless stated otherwise.

The coherent scattering intensity of SANS can be described as $I(q) = A\,P(q)S(q)$ for a monodispersed, spherical particle system, where $P(q)$ is the particle form factor and $S(q)$ is the inter-particle structure factor (the detailed description of the data analysis can be found in the supporting information). It is well known that decreasing the temperature increases the attraction strength between lysozyme proteins so that the inter-protein structure factor, $S(Q)$, is strongly temperature dependent, while the form factor, $P(Q)$, remains largely unaffected by changing solution conditions. This is confirmed by the results shown in Fig. 1 as the normalized intensities for all concentrations and temperatures overlap at high q-values. Variations in the q-dependence of normalized $I(q)$ at low q-values is therefore related to changes in inter-protein interactions.

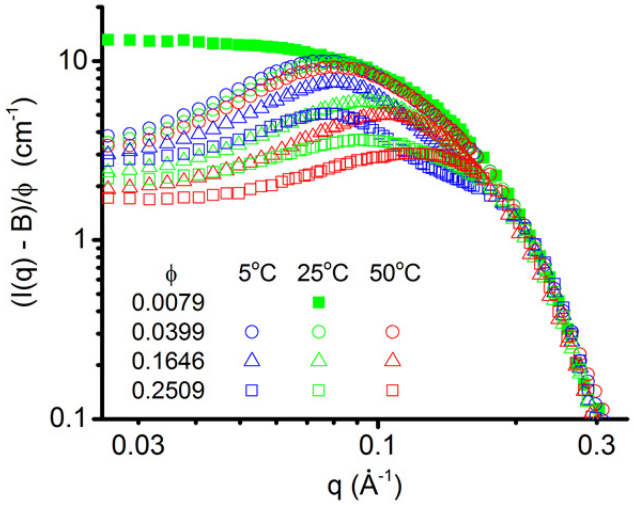

FIG. 1. Absolute scattering intensities obtained from SANS experiments scaled by their corresponding background and volume fraction are plotted for three lysozyme concentrations at three temperatures each (open symbols) along with a low concentration sample representative of the form factor (closed symbols).

Inter-protein interactions can be quantified through the analysis of $S(q)$,[16] which can be obtained by normalizing $I(q)$ by $P(q)$ and the pre-factors in the scattering equation. Shown in Fig. 2a are the extracted $S(q)$ from the experimental data for the same solution conditions as in Fig. 1 where the data are shifted vertically with increasing temperature for clarity. The most prominent feature of $S(q)$ is the formation of a low-q peak (IRO peak) at low temperatures, consistently found at ~ 0.09 Å^{-1}, for many of the solution conditions. The long-ranged electrostatic repulsion maintains overall solution homogeneity on longer length scales as indicated by small values of $S(q \approx 0)$, while short-ranged attraction drives association over shorter length scales to form a heterogenous density distribution at the intermediate range length scale. These competing forces are what drive the IRO formation.

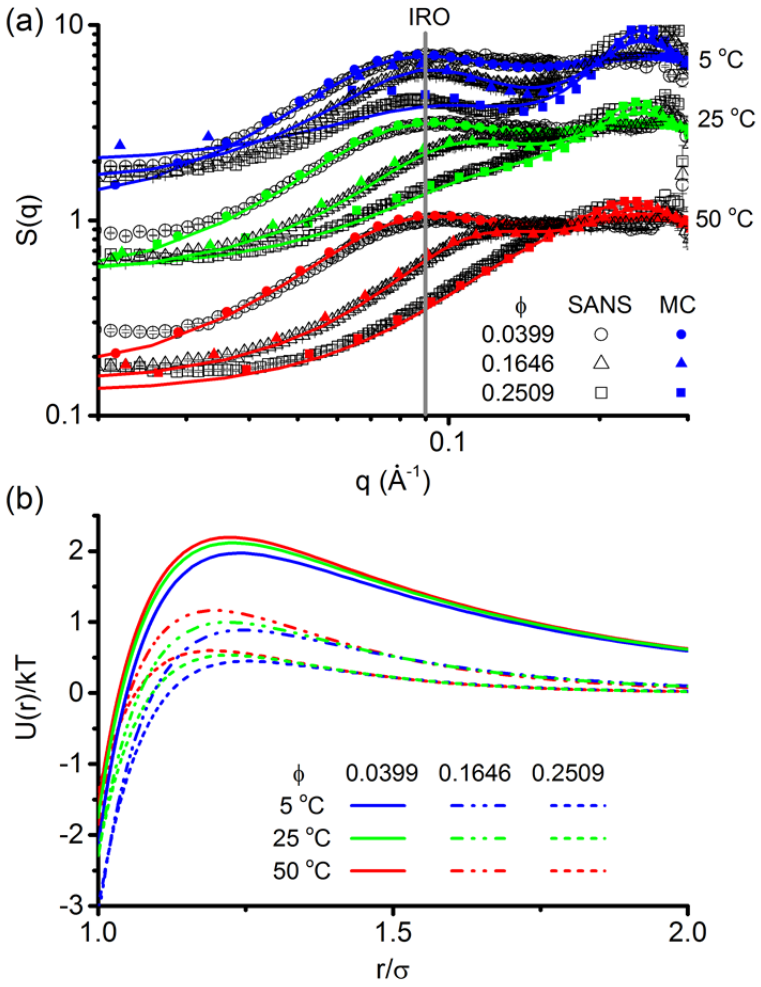

FIG. 2. (a) Inter-particle structure factors obtained from normalizing SANS data (black, open symbols) with best fits using IET (lines) and calculations from MC simulations (colored, filled symbols). All data points at 5 °C and 25 °C are shifted vertically for clarity. The solid grey line marks the q-value of IRO peak formation. (b) The interaction potentials extracted from IET fits to the SANS data shown in (a) are plotted together.

The magnitude and range of the interaction potential at different sample conditions is extracted by fitting $S(q)$ using integral equation theories (IET) for systems with the hard sphere double-Yukawa (HSDY) model,[16] where one Yukawa term is used to model the short-ranged attraction and the second Yukawa term is used to model the long-ranged electrostatic repulsion.[17,18] For the IET calculations, thermodynamic self-consistency is enforced following the previously proposed method.[16] Furthermore, the extended law of corresponding states shows that this particular choice of potential functional form of the short-ranged attraction does not matter. Equivalent structures can be obtained with different potential functional forms of the short-ranged attraction.[12] The fits to the experimental $S(q)$ are shown as solid lines in Fig. 2a, where the quality

of the fit is very good. The small deviations at higher q values are due, in part, to the experimental resolution and in part, due to possible orientation-positional coupling not accounted for in the spherical potential model.[19] The corresponding SALR interaction potentials are shown in Fig. 2b plotted as a function of center-to-center distance normalized by the particle diameter, σ. For these solutions at low ionic strength, increasing the protein concentration increases the counter-ion concentration, resulting in a decrease in the strength and range of repulsion. These HSDY potentials also show a monotonic increase in the strength of attraction with decreasing temperature.[6] During the fitting, the volume fraction of the protein is one of the fitting parameters and determines the real volume fraction of protein in solution, ϕ_{fit}. The ϕ_{fit} obtained from the SANS fitting is compared to the volume fraction calculated from the skeleton density, ϕ in Table I, where it is observed that ϕ_{fit} and ϕ are almost identical. Unfortunately, for $\phi > 0.30$, the IET does not converge and the data could not be fitted satisfactorily with the current model.

To validate our IET method, Monte Carlo (MC) simulations using the potentials from Fig. 2b are performed (details of the MC simulations are given in the supporting information). The calculated $S(q)$ of the MC simulation results (solid symbols in Fig. 2a) reproduce the $S(q)$ calculated by the IET theory (open symbols), as shown in Fig. 2a, which also shows the calculated results (solid lines). The good agreement among the MC simulation, theoretical results of the IET method, and experimental $S(q)$ from SANS provide confidence in the extracted interaction potentials.

Table I. Summary of protein volume fractions and Baxter parameters extracted from fits to the SANS data.

T (°C):		5		25		50	
conc (mg/mL)	ϕ	ϕ_{fit}	τ_B	ϕ_{fit}	τ_B	ϕ_{fit}	τ_B
10.7	0.0399	0.040	0.763	0.040	1.348	0.040	1.742
55.6	0.0800	0.077	0.245	0.077	1.087	0.074	2.774
112	0.1215	0.126	0.190	0.129	0.499	0.126	1.263
169	0.1646	0.143	0.192	0.147	0.503	0.155	0.956
230	0.2070	0.202	0.167	0.210	0.395	0.209	1.289
289	0.2509	0.239	0.184	0.240	0.428	0.244	1.328
416	0.2981		*0.183*[a]		*0.457*[a]		*1.209*[a]
480	0.3446		*0.183*[a]		*0.457*[a]		*1.209*[a]

[a] Conditions where IET fitting could not converge are italicized - τ_B values are estimated as an average of the previous four states and ϕ_{fit} is assumed to be equal to ϕ.

To locate the state points of our protein solutions in a generalized state diagram[12], we need to estimate the Baxter parameter, τ_B, from the reference attractive potential, which is defined as the attractive portion of the full interaction potential shown in Fig. 2(b). This τ_B corresponds to that of a reference attractive system whose interaction potential is simply the HS plus the reference attractive potential. ($\tau_B = 1/4(B_2^* - 1)$, where B_2^*, is the normalized second virial coefficient.[20]) Table I shows τ_B for samples over the range of protein concentrations and temperatures. It is noted that for $0.10 < \phi < 0.3$, τ_B does not change significantly upon increasing the concentration. This is clearer when plotting τ_B as a function of ϕ (solid

symbols) shown in Fig. 3. Therefore, it is reasonable to speculate that for samples at even higher concentrations, τ_B would not vary significantly. Hence, for $\phi > 0.30$, τ_B was estimated as the average value of the four points for the volume fraction between 0.1 and 0.3.

With known values of τ_B and ϕ, all experimental state points (solid circles) are located on the generalized phase diagram shown in Fig. 3. Note that the state points for $\phi > 0.30$ are distinguished as open symbols. As a comparison, we also draw the binodal (gray solid line) and percolation line (long dashed line) for the reference attractive hard sphere (AHS) system. Based on the previously proposed generalized phase diagram of the SALR system, the region above the binodal line of the reference AHS system has two different types of states that are separated by the percolation line of the SALR system. The state points on the left of the percolation line are in the dispersed fluid state (blue horizontal solid lines), while the state points on the right of the percolation line are in the random percolated state (green solid vertical lines)

The percolation line (black short dashed line) of our lysozyme samples is estimated based on previous MC simulations on systems with similar competing interactions, and is known to occur at smaller volume fractions relative to the percolation line of purely attractive systems.[21] We also performed MC simulations to estimate the onset of percolation, the results of which also agree with the short dashed solid line (see the Supporting Information).

The states of most of the lysozyme samples (solid ciricles shown in Fig. 3) are in the dispersed fluid state. For higher concentrations, some of them are in the random percolated state. As defined in previous work,[12] dispersed fluids are equilibrium states consisting of a polydisperse distribution of monomers and clusters and random percolated states contain a system spanning network. Since all of our state points are above the binodal line of the reference AHS system, none of the lysozyme samples have clusters with a dominant, preferred size even though some of them show a strong, clear IRO peak in $S(q)$ as shown in Fig. 2.

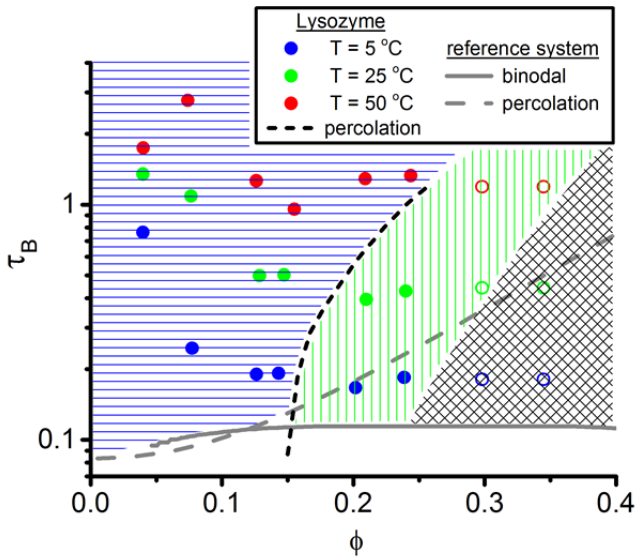

FIG. 3. State diagram of lysozyme showing state points plotted relative to the AHS binodal (grey line) and percolation transition (long dashed line). States transition from a dispersed fluid (blue horizontal lines) to a dynamically percolated state (green vertical lines) and finally to a locally glassy state (black hatched lines) with increasing volume fraction. Open symbols denote state points for which τ_B is estimated.

Samples with the localized glass behavior are identified from the mean square displacement (MSD), $\langle R^2 \rangle$, as calculated from the NSE data.[22] Previous NSE measurements of the intermediate scattering function for our lysozyme solutions were analyzed to obtain $\langle R^2 \rangle$.[13] The MSDs are normalized by the particle diameter, $\langle R^{*2} \rangle = \langle R^2 \rangle / \sigma^2$, as a function of dimensionless time, $t^* = t/t_D$, where t_D is the characteristic time of diffusion defined as $t_D = 3\pi\eta_S\sigma^3/4k_BT$, with k_BT the thermal energy, and η_S the solvent viscosity. Table S1 in the supporting information contains a summary of t_D values for lysozyme as a function of temperature. The normalized MSDs of lysozyme samples have been previously obtained and are now replotted in Fig. 4.[13] On the same figure are plotted the dynamic transition lines observed in colloidal systems using confocal microscopy by directly measuring MSDs of the particles.[11] The localized glassy state points of our samples are identified as having MSDs that lie below this glass transition line.[11] It is important to note, however, that our lysozyme samples are all Newtonian fluids in the long time limit, such that the small MSDs we observed are due to *localized* glassy behavior.[13] The state points with this locally glassy behavior are identified in this manner, and are shown in the state diagram as the region with crosshatched lines in Fig. 3.

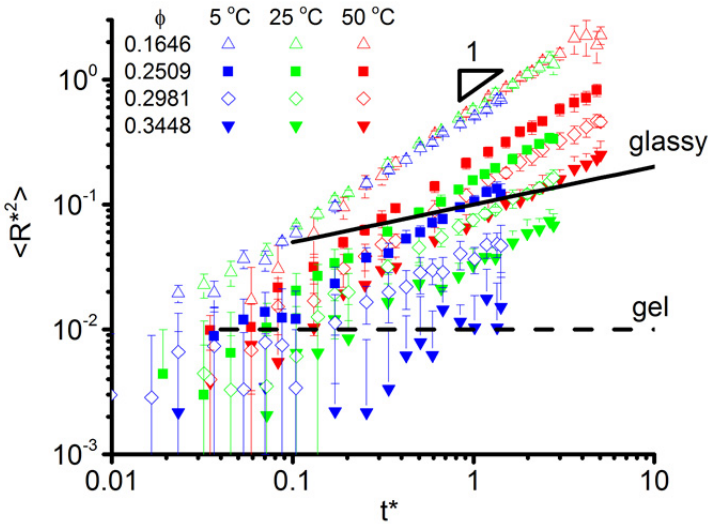

FIG. 4. Mean squared displacements of lysozyme samples normalized by the particle diameter (obtained from NSE) are plotted with results obtained previously for micron sized particles (lines) as a function of the normalized time (see text).

Not unexpectedly, the states with this localized glassy behavior lie well inside the percolation line for lysozyme. When the volume fraction is just slightly over the percolation transition, proteins remain mobile at both local and macroscopic scales. By further increasing the protein concentration, the absolute magnitudes of the MSDs quickly decrease and eventually are below that of previously reported glassy behavior in systems with competing interactions over the full range of time scales studied, which we defined here as localized glassy states. The attraction drives the heterogenous density distribution resulting in glassy behavior at the intermediate length scale. The presence of long-ranged repulsion in solution confines the glassy state locally and maintains a relatively mobile configuration of the whole system at long time scales.

By further increasing the protein concentration, a macroscopic glass transition can occur. It is likely that the protein concentration necessary for macroscopic glass formation will approach the volume fraction of locally dense regions, which was estimated previously to be about 0.40 by both simulation[12] and experiment.[9] It is also very interesting to point out that the most dynamically retarded locally glassy state studied here ($\phi = 0.35$, T = 5 °C) surpasses already the Löwen criterion for freezing (see the Supporting Information).[23] The IRO driven by the SALR potential may therefore introduce some special dynamic features. Recently, it has been also shown that some colloidal glass systems can be understood through a critical-like behavior, which is linked to medium-range crystalline order.[24] It will be extremely interesting to test this in an SALR system in future.

To summarize, we have studied the interaction potential between lysozyme solutions and identified the region of localized glassy dynamics in the generalized phase diagram with competing interactions. The location of the transition in

phase space is consistent with an early study that dynamic percolation is a necessary, but not sufficient requirement for the onset of glassy behavior in systems with short-ranged attraction and long-ranged repulsion.[15] Before the whole system transitions to a glassy state, glassy like behavior can be found for particles at the intermediate range length scale. However, the long time dynamics is still relatively fast and lead to the Newtonian behavior of the system due to the presence of the long range repulsion. These results provide the first quantitative connection between the interaction potential of an SALR system and the expected onset of localized glassy behavior. The state diagram presented here provides significant progress in our understanding of gelation and glassy behavior in soft matter materials with the competing interactions and aids in our general understanding of glass transitions of (near) spherical colloidal systems.

Supplmenary Material

See supplementary material for the sample preparation, SANS fitting methods and results, Monte Carlso simulation methods and results, characterstic diffusion time of lysozyme at different temperatures, and NSE results.

Acknowledgements

This manuscript was prepared under cooperative agreements 70NANB12H239 and 70NANB10H256 from NIST, U.S. Department of Commerce. This work utilized facilities supported in part by the National Science Foundation under Agreement No. DMR-1508249. Certain commercial equipment, instruments, or materials are identified in this document. Such identification does not imply recommendation or endorsement by the National Institute of Standards and Technology nor does it imply that the products identified are necessarily the best available for the purpose.

Refereces:

[1] A.P.R. Eberle, R. Castañeda-Priego, J.M. Kim, and N.J. Wagner, Langmuir **28**, 1866 (2012).

[2] A.P.R. Eberle, N.J. Wagner, and R. Castañeda-Priego, Phys. Rev. Lett. **106**, 105704 (2011).

[3] W.B. Russel, N.J. Wagner, and J. Mewis, J. Rheol. **57**, 1555 (2013).

[4] N.E. Valadez-Pérez, Y. Liu, A.P.R. Eberle, N.J. Wagner, and R. Castañeda-Priego, Phys. Rev. E **88**, 060302(R) (2013).

[5] E. Zaccarelli, J. Phys. Condens. Matter **19**, 323101 (2007).

[6] A.C. Dumetz, A.M. Chockla, E.W. Kaler, and A.M. Lenhoff, Biophys. J. **94**, 570 (2008).

[7] D. Rosenbaum, P. Zamora, and C. Zukoski, Phys. Rev. Lett. **76**, 150 (1996).

[8] N.E. Valadez-Pérez, A.L. Benavides, E. Schöll-Paschinger, and R. Castañeda-Priego, J. Chem. Phys. **137**, 84905 (2012).

[9] A. Campbell, V. Anderson, J.S. van Duijneveldt, and P. Bartlett, Phys. Rev. Lett. **94**, 208301 (2005).

[10] F. Sciortino, P. Tartaglia, and E. Zaccarelli, J. Phys. Chem. B **109**, 21942 (2005).

[11] C.L. Klix, C.P. Royall, and H. Tanaka, Phys. Rev. Lett. **104**, 165702 (2010).

[12] P.D. Godfrin, N.E. Valadez-Pérez, R. Castañeda-Priego, N.J. Wagner, and Y. Liu, Soft Matter **10**, 5061 (2014).

[13] P.D. Godfrin, S.D. Hudson, K. Hong, L. Porcar, P. Falus, N.J. Wagner, and Y. Liu, Phys. Rev. Lett. **115**, 228302 (2015).

[14] L. Porcar, P. Falus, W.-R. Chen, A. Faraone, E. Fratini, K. Hong, P. Baglioni, and Y. Liu, J. Phys. Chem. Lett. **1**, 126 (2010).

[15] F. Cardinaux, E. Zaccarelli, A. Stradner, S. Bucciarelli, B. Farago, S.U. Egelhaaf, F. Sciortino, and P. Schurtenberger, J. Phys. Chem. B **115**, 7227 (2011).

[16] J.M. Kim, R. Castañeda-Priego, Y. Liu, and N.J. Wagner, J. Chem. Phys. **134**, 64904 (2011).

[17] Y. Liu, W.-R. Chen, and S.-H. Chen, J. Chem. Phys. **122**, 44507 (2005).

[18] S.-H. Chen, M. Broccio, Y. Liu, E. Fratini, and P. Baglioni, J. Appl. Crystallogr. **40**, s321 (2007).

[19] E.J. Yearley, P.D. Godfrin, T. Perevozchikova, H. Zhang, P. Falus, L. Porcar, M. Nagao, J. Curtis, P. Gawande, R. Taing, I.E. Zarraga, N.J. Wagner, and Y. Liu, Biophys. J. **106**, 1763 (2014).

[20] M. Miller and D. Frenkel, J. Chem. Phys. **121**, 535 (2004).

[21] N.E. Valadez-Pérez, R. Castañeda-Priego, and Y. Liu, RSC Adv. **3**, 25110 (2013).

[22] W. van Megen, T. Mortensen, S. Williams, and J. Müller, Phys. Rev. E **58**, 6073 (1998).

[23] H. Lowen, T. Palberg, and R. Simon, Phys. Rev. Lett. **70**, 1557 (1993).

[24] H. Tanaka, T. Kawasaki, H. Shintani, and K. Watanabe, Nat. Mater. **9**, 324 (2010).

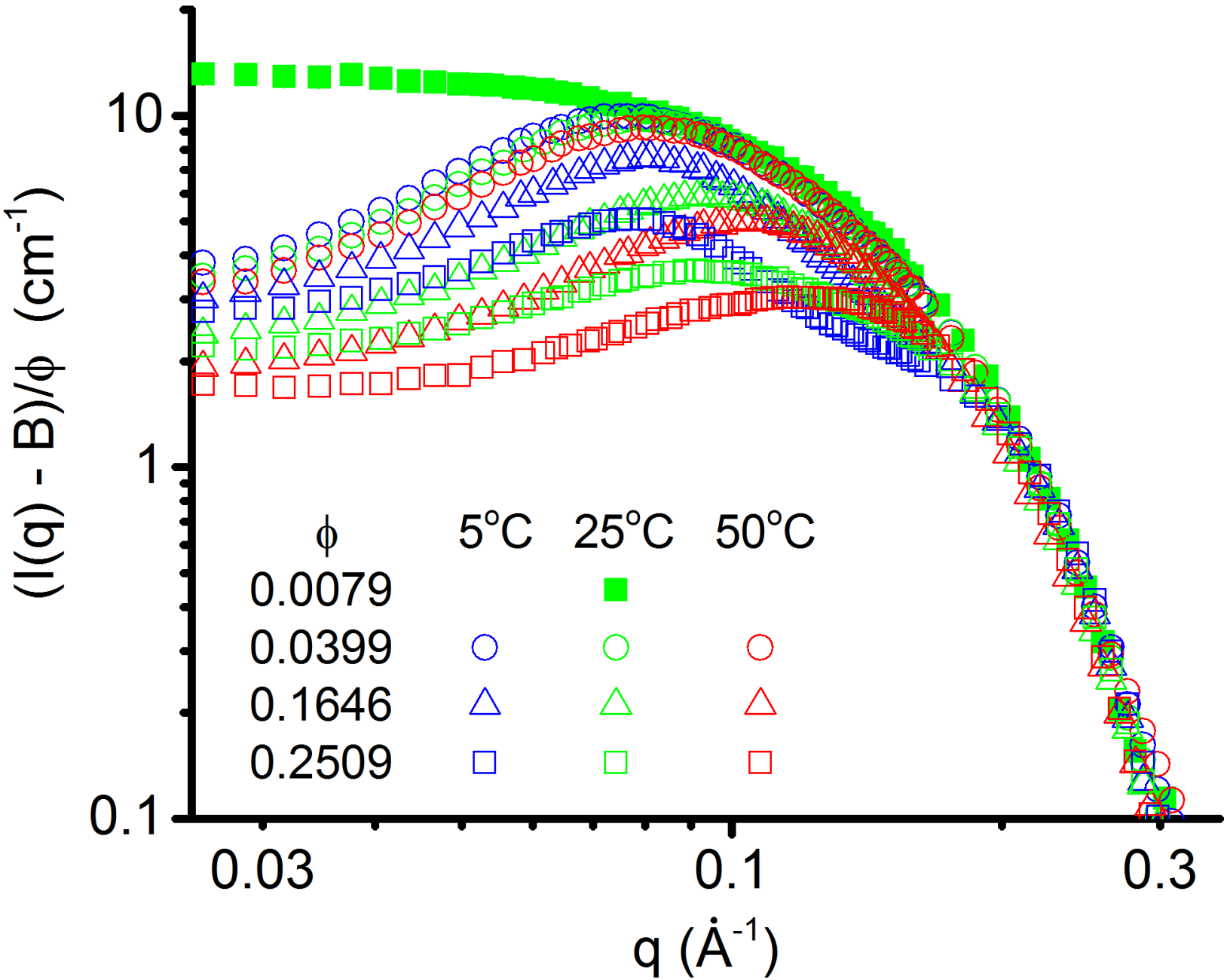
10
1
0.1
(I(q) - B)/ϕ (cm-1)
ϕ
5°C
25°C
50°C
0.0079
0.0399
0.1646
0.2509
0.03
0.1
0.3
q (Å-1)

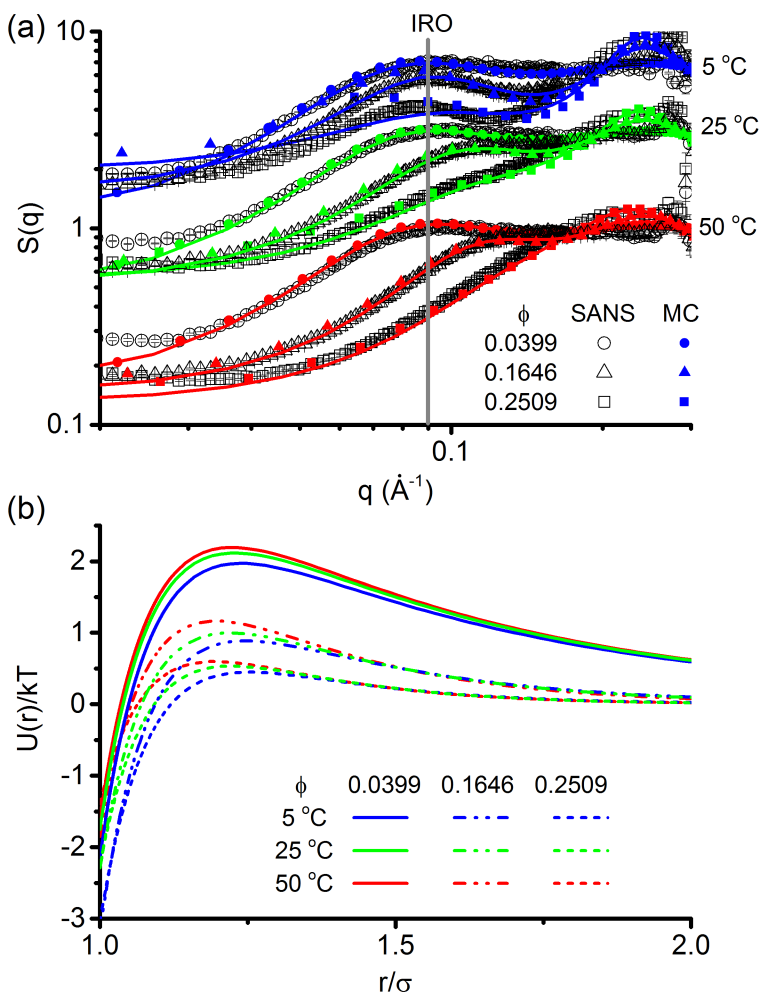
(a)
IRO
5 °C
25 °C
50 °C
S(q)
10
1
0.1
0.1
q (Å^{-1})
ϕ SANS MC
0.0399
0.1646
0.2509
(b)
U(r)/kT
2
1
0
-1
-2
-3
ϕ 0.0399 0.1646 0.2509
5 °C
25 °C
50 °C
1.0
1.5
2.0
r/σ

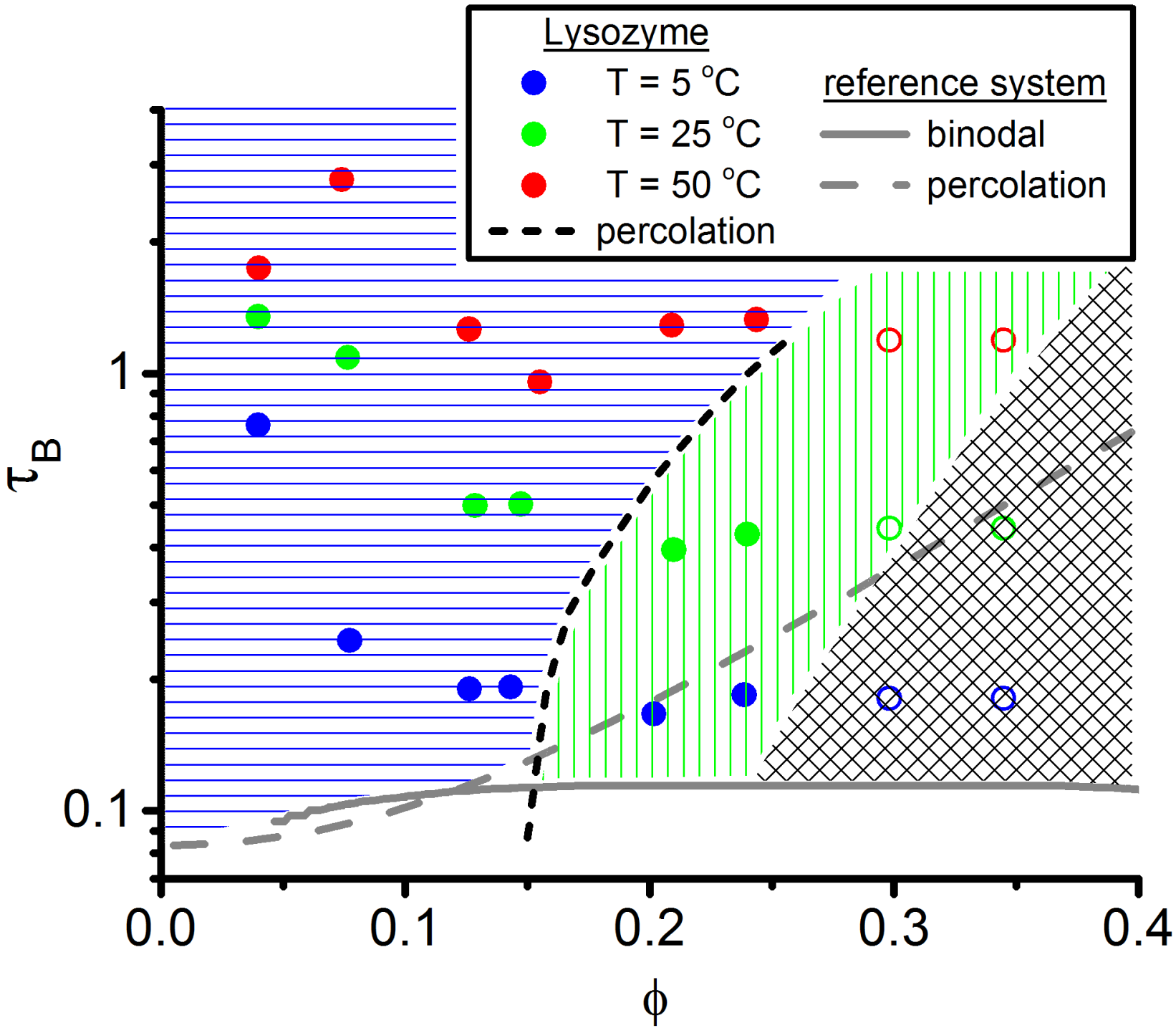
Lysozyme
T = 5 °C
T = 25 °C
T = 50 °C
percolation
reference system
binodal
percolation
1
0.1
τ_B
0.0
0.1
0.2
0.3
0.4
ϕ

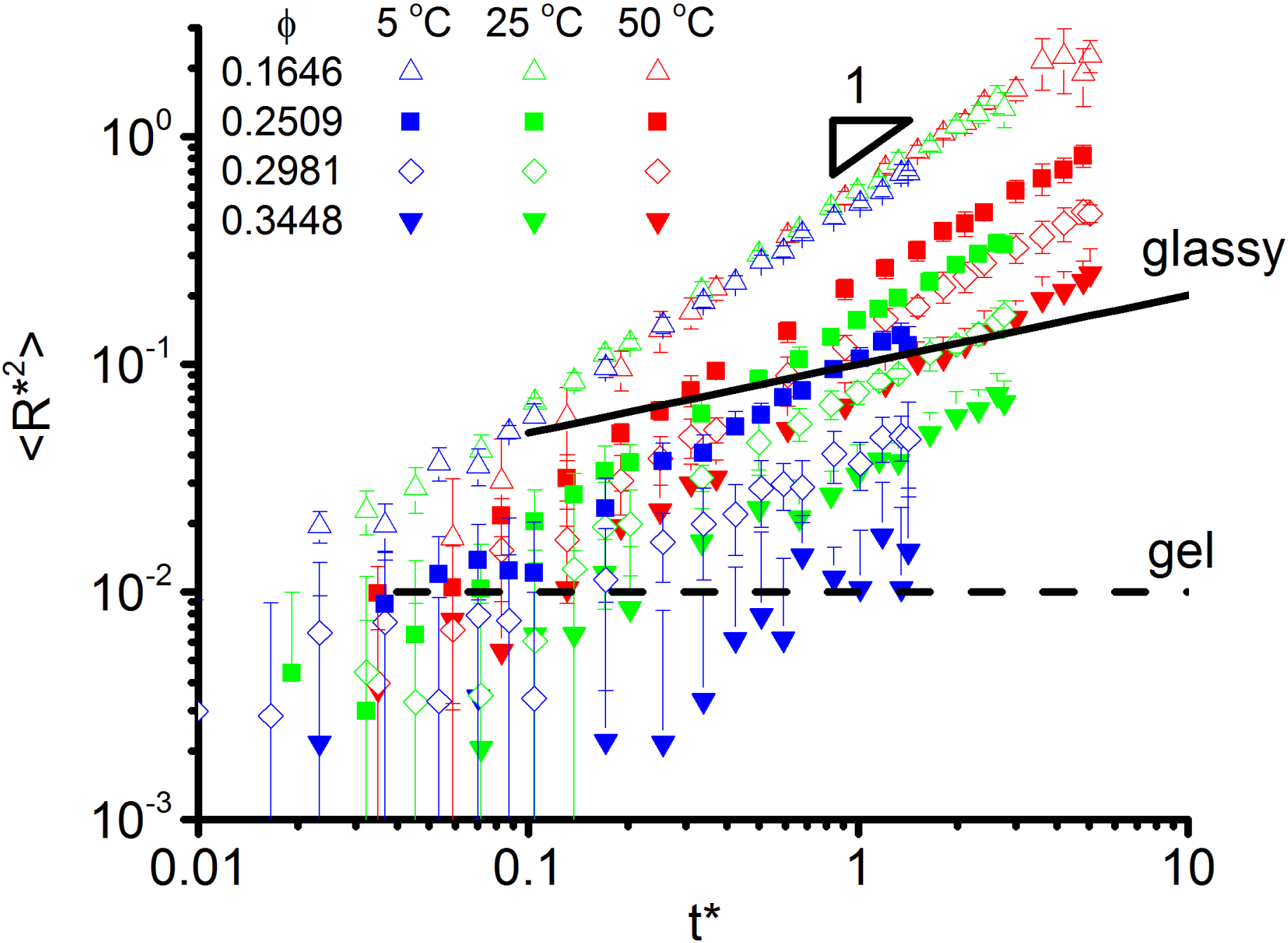
ϕ
5 °C
25 °C
50 °C
0.1646
0.2509
0.2981
0.3448
1
glassy
gel
<R*²>
10⁰
10⁻¹
10⁻²
10⁻³
0.01
0.1
1
10
t*